Pure & Appl. Chem., Vol.53, pp.1277-1290.
Printed in Great Britain.

0033-4545/81/061277-14$02.00/0
Pergamon Press Ltd

ASPECTS OF STRUCTURE IN IONIC SOLUTIONS

Harold L. Friedman

Department of Chemistry, S.U.N.Y., Stony Brook, New York 11794, U.S.A.

Abstract - Several aspects of model calculations in solution theory are discussed in connection with three recent developments. These concern the structural aspects of ion pairing, the indications of lattice structure in concentrated $NiCl_2$ solutions, and the characteristics of solvent-averaged ion-ion potentials deduced from models in which both the solvent and the ions are represented in molecular detail.

INTRODUCTION

The theory of structure and dynamics in solutions is now entering a phase of remarkably fast and widespread development. There is an atmosphere of great excitement because the new developments promise to resolve the paradoxes and obscurities which delight and charm solution chemistry experts like us, but which make it so difficult to arrive at unique molecular interpretations of solution phenomena. As H. S. Frank said (1) "....there has been no dearth of ingenious suggestions about what water *might* be like in order to display this or that set of properties, (but) it is only recently, by use of new experimental techniques and by applying data and interpretations from several fields, that it has begun to be possible to draw useful inferences about what water *must* be like...." I think that this view of the problem of understanding water and aqueous solutions equally well indicates the character of the problems in the wider field of solution chemistry.

Now I would like to discuss three recent theoretical developments which relate to the equilibrium structure in ionic solutions and which promise to lead from "might be" to "must be". They are chosen to illustrate the power of the methods that are now available to those who study the theory of solutions. It should be remarked that unfolding theoretical developments concerning rate processes in solution, which are, if possible, even more exciting, have been described in an important review by P. G. Wolynes (2). We also remark that the primary source of structural information is experiment rather than theory, but in these solution problems, perhaps more than in any others, the accurate interpretation of experimental data depends upon application of theory.

In discussing the theoretical developments I find it helpful to refer to certain classes of models. The word 'model' now is often used to mean a set of approximations of any kind, so it is convenient to use the term Hamiltonian model to mean a physical model. The model's Hamiltonian specifies the forces acting upon each particle in each possible configuration of the system, i.e. each set of locations of all of the particles. This may be done at several levels as summarized in Table 1 (3,4,5). From each kind of model one can calculate the equilibrium structure of the solution at a level of detail corresponding to the model, also as indicated in Table 1.

The most widely used measure of structure in fluids is the pair correlation function (3-10) (or radial distribution function) $g_{ij}(r)$. It is defined so that

$$c_{i/j}(r) = c_i \, g_{ij}(r) \qquad (1)$$

is the local concentration of particles of species i in a small volume at a distance r from the center of a particle of species j. Also $c_i=N_i/V$ is the bulk or stoichiometric concentration of species i. At small r, one has $g_{ij}(r)=0$ because the particles each occupy space from which other particles are excluded, basically because of the Pauli exclusion principle. Values of g_{ij} greater than unity reflect attraction between i and j, while values less than unity reflect repulsion. Indeed the potential $w_{ij}(r)$ of the average force between i and j in the fluid is given by the equation

TABLE 1. Hamiltonian models for solutions

LEVEL	PARTICLES	MECH.[a]	STRUCTURE FUNCTIONS[b]
S , SCHRÖDINGER	NUCLEI, ELECTRONS	Q	$\Psi(q_n,q_e)$
BO, BORN-OPPENHEIMER	NUCLEI: IONS & SOLVENT	C	$g_{ij}(X_i,X_j)$
MM, McMILLAN-MAYER	IONS ONLY	C	$g_{ij}(r)$

$H \xrightarrow[\text{SOME APPROXIMATION METHOD}]{} [\Psi \quad \text{or} \quad g] \longrightarrow$ MEASURABLE PROPERTY

[a] Q: quantum mechanics is required. C: classical mechanics is sufficient.

[b] It is indicated that the wave function Ψ depends upon the coordinates q_n of the nuclei and the coordinates q_e of the electrons. The remaining notation is explained in the text.

$$g_{ij}(r) = e^{-w_{ij}(r)/k_BT} \tag{2}$$

where k_B is Boltzmann's constant and T the temperature.

If the functions g_{ij} for all of the species pairs in a fluid are known over a sufficient range of the state variables, one can calculate the thermodynamic properties (3,6-10). So forces determine structure through Eq. (2) and the thermodynamic properties are determined by the structure.

In the case of a solution, the potential w_{ij} is not generally the potential of the force acting between particles i and j in a vacuum, or even at infinite dilution in the solvent. Rather it is the potential of the average force between particles i and j in the medium in which g_{ij} is measured. In this case the force is mediated by all of the other particles.

At the deepest level in Table 1, the Schroedinger level, the Hamiltonian is well known. Quantum mechanics must be used to calculate the wave functions Ψ which carry the information about the structure of the system.

Among the functions one can, at least in principle, calculate at the Schroedinger level is the Born-Oppenheimer (BO) potential surface, the potential of the forces among the nuclei assuming that at each nuclear configuration the time-independent Schroedinger equation is satisfied. We may think of this as the 'electron-averaged' potential. Such an N-body potential U_N may be adequately represented as a sum of pair potentials

$$U_N(\vec{r}_1, \vec{r}_2, \cdots, \vec{r}_N) = \sum_{\text{pairs}} u_{ij}(r_{ij}) \tag{3}$$

where the particle indices in the pair potentials may pertain to monatomic particles or to molecules; in the latter case the coordinates must in general include orientational and other internal coordinates as well as the center-to-center distance r_{ij}. Thus in Table 1 in $g_{ij}(X_i, X_j)$ the symbol X_i denotes the full set of coordinates for particle i.

The program of calculating the BO-level potentials from the Schroedinger level cannot often be carried through with the accuracy required for the intermolecular forces in solution theory (11-13). Fortunately a great deal can be learned about liquids through the study of BO-level models in which the N-body potential is pairwise additive (as in Eq. (3)) and in which the pair potentials have very simple forms (7-9). Thus for the hard sphere fluid we have, with σ=sphere diameter,

$$\begin{aligned} u(r) &= \infty \quad \text{if} \quad r<\sigma \\ &= 0 \quad \text{if} \quad r>\sigma \end{aligned} \tag{4}$$

while for the 6-12 fluid we have

$$u(r) = e_0[(\sigma/r)^{12}-2(\sigma/r)^6] \tag{5}$$

The 6-12 potential is not quantitatively like the realistic potentials that can be derived by calculations at Schroedinger level for, say, Ar-Ar interactions. But it requires careful and detailed study to see how real simple fluids (i.e. one component fluids with monatomic particles) deviate from the behavior calculated from the 6-12 model. Moreover, the structure factor of the dense 6-12 fluid can be fit with amazing accuracy by the structure factor of a hard sphere fluid of appropriate density and diameter (7). The structure factor $S_{ij}(k)$ is essentially the Fourier transform of the pair correlation function: in general we define the dimensionless structure factor S'(k) as

$$S'_{ij}(k) = (\rho_i\rho_j)^{1/2} \int_0^\infty 4\pi r^2 dr[g_{ij}(r)-1]\cdot \frac{\sin kr}{kr} + 1 \tag{6}$$

where $\rho_i=N_i/V$ is the particle number density for species i. The structure factor is important because it is simply related to the density of scattered radiation in a diffraction experiment (7,8).

The lesson, that drastically simple Hamiltonian models are adequate to generate quite realistic fluid properties and hence to understand the structure of fluids, can be reinforced by many other examples. For the present discussion the most important may be the Stillinger-Rahman series of studies of a BO-level Hamiltonian model for water (14).

In a McMillan-Mayer level model (MM-level) for a solution, the particles are the solute particles (i.e. the ions with positive, negative, or zero charge) (3,15). The ion-ion potentials can, in principle, be generated by calculations in which one averages over the solvent coordinates in a model at BO level, in which the solvent particles are explicitly represented. Pairwise additivity (we use overbars for solvent-averaged potentials)

$$\bar{U}_N(\vec{r}_1, \vec{r}_2,\cdots,\vec{r}_N) = \sum_{\text{pairs of ions}} \bar{u}_{ij}(r_{ij}) \tag{7}$$

is not so accurate or realistic as at the BO-level, but inconsistencies due to the neglect of higher terms have not appeared to date, although recently it has been discovered that the neglected terms include some long-range interactions (cf. Section IV).

The simplest model for ionic solutions at the MM-level is the primitive model, (3,16,17)

$$\bar{u}_{ij} = u_{ij}^{HS} + e_ie_j/\varepsilon r \tag{8}$$

where u_{ij}^{HS} is the potential given in Eq. (4), with $\sigma\to\sigma_{ij}$, and where ε is the dielectric constant of the solvent medium. This is implicitly the model studied by Debye and Hückel, and in most later studies of ionic solution theory as well. The well known Debye-Hückel result for the potential of average force,

$$w_{ij}(r) = u_{ij}^{HS}(r) + e_ie_je^{-\kappa r}/\varepsilon r , \tag{9}$$

where κ^{-1} is the Debye shielding length, is not very accurate, even for this model, compared to some of the later results.

In Table 1 it is indicated that, to deduce the pair correlation functions for a given model from the Hamiltonian, one employs some approximation method. At the BO or MM level the simulation methods MD (Molecular Dynamics (7,8,18)) and MC (Monte Carlo (7,8,19)) are very reliable, as long as all of the technical details are carefully handled, but they are relatively expensive and imprecise. There are many other approximation methods, some mentioned below, but the most generally useful for the work reviewed here is the HNC (hypernetted chain integral equation) method (3,7,8).

SECTION II - ION PAIRS

We begin by looking at ion pairing in the context of a corresponding states diagram (Fig. 1) (20). Here the reduced temperature T_r is given by

$$T_r = R/b \tag{10}$$

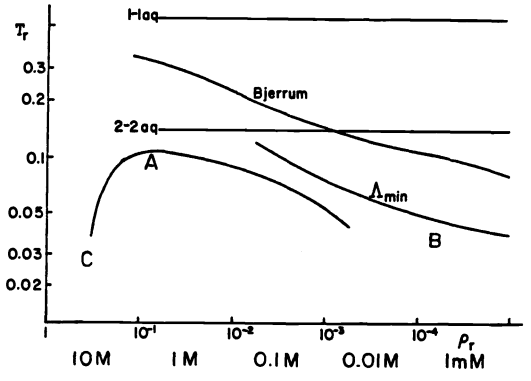

Fig. 1. The corresponding states diagram for the ionic fluid (20). Curve A is the coexistence line estimated for the restricted primitive model. In the region under the coexistence line the dilute ionic system on the right is in phase equilibrium with the more concentrated ionic system on the left. Region B is typical for dilute ionic solutions in weakly polar solvents while region C is typical for fused salts. The line 1-1 aq (2-2 aq) is the locus of equilibrium states of a typical 1-1 (2-2) electrolyte in water assuming that the minimum in the solvent-averaged pair potential $\bar{u}_{+-}(r)$ is near r=R=4Å. The curve labelled Bjerrum is the locus of states in which the ions are 50% paired according to his theory, while Λ_{min} is the locus of the conductivity minimum according to the usual triple ion theory. The lowermost scale is approximately the stoichiometric molarity if the ions are spheres with 4Å diameter.

where R is the location of the minimum in $\bar{u}_{+-}(r)$, and b is the Bjerrum length,

$$b = |e_+e_-|/\varepsilon k_B T \tag{11}$$

where e_i is the ionic charge, and ε the dielectric constant of the solvent. The reduced particle number density

$$\rho_r = (4\pi/3)(\rho_+ + \rho_-)(R/2)^3, \tag{12}$$

is the fraction of the space occupied by the ions, if they have equal sizes. The coexistence curve in Fig. 1 is a characteristic of ionic media that is not well understood (20).

The Bjerrum line in Fig. 1 is the locus of states where, according to Bjerrum's 1926 theory (21) for a symmetric binary electrolyte, (e_+=-e_-) half of the ions are paired and half are free.

The phenomena related to ion pairs have been studied (21,22,23) using the simplest MM-level model, the primitive model, for which the pair potential is given in Eq. (8). If one chooses R=4.2Å, and the other parameters appropriate for a 2-2 aqueous electrolyte at 25°C (or, equally, for a 1-1 electrolyte with ε≈20) then $T_r \sim 0.15$ and it is evident from Fig. 1 that this isotherm crosses the Bjerrum line. In order to shed further light on this problem we also have studied the closely related charged soft sphere model, for which the potential is given by

$$\bar{u}_{ij}(r) = B_{ij}\cdot[r_i^* + r_j^*)/r]^n + e_ie_j/\varepsilon r \tag{13}$$

with

$$B_{ij} = A_m|e_ie_j|/6n[r_i^* + r_j^*] \tag{14}$$

where A_m is the Madelung constant, 6 the coordination number, and r_i^* the nominal radius of an ion of species i. This term is so constructed that in a close-packed electrically neutral binary crystal, the nearest-neighbor distance calculated from Eq. (13), with ε=1, will be $r_+^* + r_-^*$; hence these parameters have the significance of crystal radii. For n=9, ε=78.358, and $r_+^* = r_-^* = 1.4778$Å, one finds from Eq. (13) that the minimum in $\bar{u}_{+-}(r)$ is at r=R=4.2Å. Accurate calculations for this soft sphere model show (22) that it gives thermodynamic

properties and structure that agree closely with the much studied (20,23) primitive model with diameters R=4.2Å.

Figure 2 shows the osmotic coefficients ϕ calculated for primitive and charged soft sphere models by the HNC equation and several other approximation methods. A special technique for the required fast Fourier transforms was used to get HNC solutions for the soft sphere model that are accurate in very dilute solutions (24). It is apparent that the Eq. (8) and (13) models do agree very closely, judging by the HNC results. The deviation between the soft sphere and primitive models at very low concentration is attributed to inaccuracy in the calculation for the latter, which did not employ the new FFT technique.

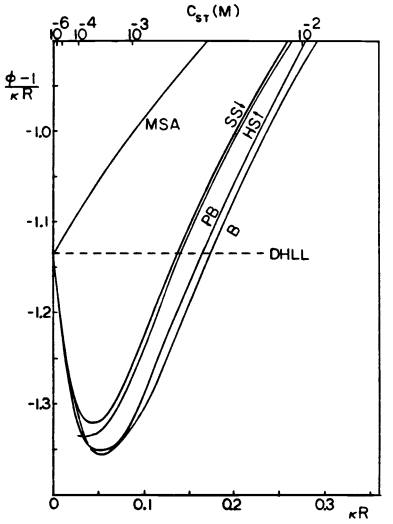

Fig. 2. Osmotic coefficients ϕ for models for a 2-2 aqueous electrolyte (24). c_{st} is the stoichiometric molarity and κ is the Debye kappa. The DHLL line is the limiting law for the function plotted. The other approximations for the primitive model are MSA, the mean spherical approximation, HS, the HNC approximation, PB, the full Poisson Boltzmann equation, and B, Bjerrum's chemical model. The HNC approximation for a charged soft-sphere model is labelled SS. In each case R=4.2Å is the location of the minimum in $\bar{u}_{+-}(r)$.

The results in Fig. 2 also show that the Bjerrum approximation gives as good results as the much more elaborate non-linear Poisson-Boltzmann equation approximation. The latter deviates noticeably from the HNC approximation even at extremely low concentrations (24). On the other hand Monte Carlo results, not shown here, agree very well with the HNC results (25).

With this background for the osmotic coefficient behavior of the models, as investigated in various ways, we may turn to computed values of structural quantities for the primitive model. In Fig. 3 we show values of g_{+-} and g_{++} at contact (where r≡R) as functions of c_{st}, the number of moles of the electrolyte per liter of solution. By DH we mean the approximation

$$g_{\substack{+-\\++}}(r) = \exp(\pm b e^{-\kappa r}/r) \qquad (15)$$

which, if linearized, corresponds to the limiting law $\ln \gamma_{\pm} = -\frac{1}{2} b\kappa$ and by DHEXT we mean the approximation

$$g_{\substack{+-\\++}}(r) = \exp\left(\pm \frac{b}{r(1+\kappa R)} e^{-\kappa(r-R)}\right) \qquad (16)$$

which, if linearized, corresponds to the extended DH equation $\ln \gamma_{\pm} = -\frac{1}{2} b\kappa/[1+\kappa R]$. Looking first at $g_{+-}(R)$ in Fig. 3 it is remarkable that DHEXT and even DH are about as good as the modern approximation EXP (7-10) judging by agreement with HNC, while Bjerrum's approximation for g_{+-} is better yet. Actually Bjerrum calculated only thermodynamic quantities, but it was recently found to be possible to extract the g_{+-} correlation function

$$g_{+-}(r) = (\alpha/K\rho_{+}) e^{b/r} \quad \text{for} \quad r \leq b/2 \qquad (17)$$

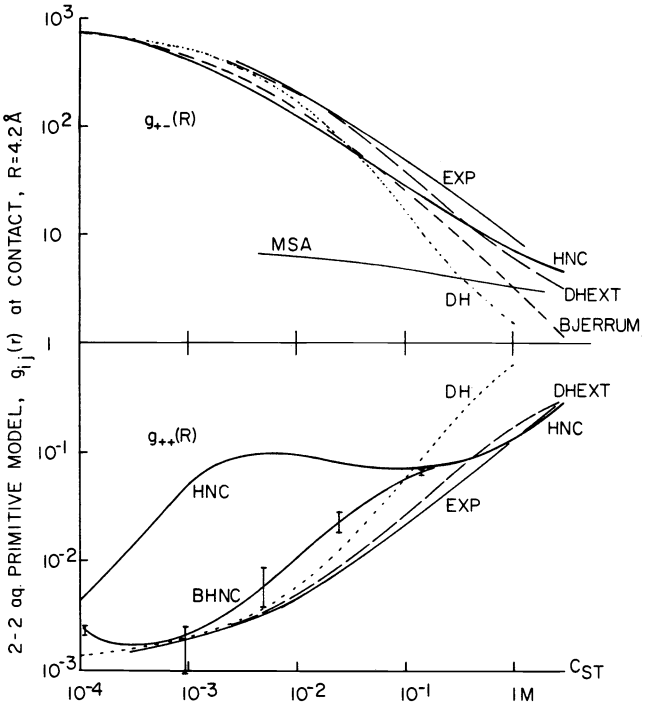

Fig. 3. Values of correlation functions for +- and ++ pairs at contact (i.e. r=R) for primitive model for 2-2 aqueous electrolytes (22). The curves are labelled by the approximation used, as described in the text.

from Bjerrum's theory by functional differentiation (26). Here K is the Bjerrum mass action constant and α is the fraction of ions that are paired, by his criteria. Eq. (17) gives the Bjerrum curve in Fig. 3.

In view of the remarkable success of Bjerrum's theory judged by the osmotic coefficients as well as contact values of $g_{+-}(r)$, it is interesting to remark that Eq. (17) shows that $g_{+-}(r)$ implied by Bjerrum's theory merely shifts up or down as one changes the concentration, which enters only through α. This is in contradiction to the prediction of more accurate theory, according to which $g_{+-}(r)$ changes shape when the concentration is changed (25,26).

Even at concentrations as low as c_{st}=0.001M the various estimates of $g_{+-}(R)$ differ by 5 or 10% (26,27). This fact tends to cloud the interpretation of conductivity and other data in which approximations weaker than the HNC have been used. On the other hand, it would be highly interesting to find an experimental technique that is especially sensitive to $g_{+-}(R)$, rather than to correlations at larger distances (cf. Eq. (21) below, and discussion).

The comparison of various results for $g_{++}(R)$, also in Fig. 3, shows a remarkable non-uniformity in the HNC estimate. This was first found for the primitive model (23) and then confirmed (27); it also is found for charged soft spheres (22). However, it turns out to be a defect of the HNC approximation that gives this enormous enhancement of ++ pairs. As established by comparison with Monte Carlo calculations, the actual enhancement is much smaller (22). It is reflected in the curve for the BHNC approximation shown in Fig. 3. For the primitive model BHNC calculation in Fig. 3 it was assumed that $g_{ij}^{BHNC} = g_{ij}^{HNC} \exp s'_{ij}$ where s'_{ij} is a sum of 'bridge graphs' (also called elementary diagrams) calculated by Rossky et. al. for the soft sphere model (22).

The considerable excess of ++ pairs which the BHNC approximation shows relative to the others is due to clusters of 3 or 4 ions. This was surmised on the basis of the behavior of $g_{++}(r)$ as a function of r (25,27) and has been confirmed by Monte Carlo calculations, from which one can extract 3 point and higher correlations as well as merely pair correlations (22). The results are shown in Fig. 4. Apparently at 0.005M only a relatively small proportion of ++ pairs are due to two cations that are near to each other but relatively far from all other cations. Evidence for such larger-than-pair clusters at low concentrations has also been found in some experimental systems (28,29) but this is the first quantitative determination

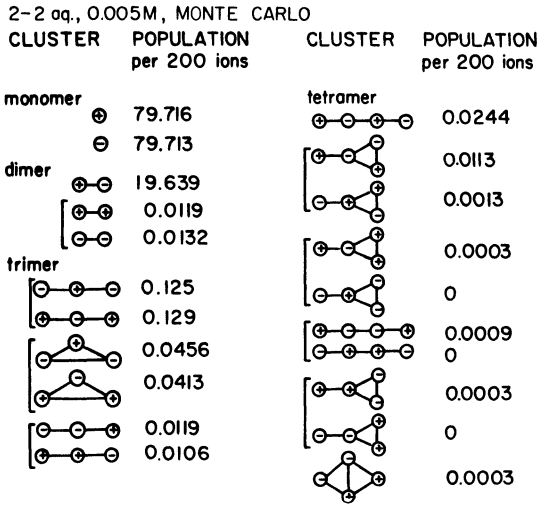

Fig. 4. Cluster populations for 2-2 aq. charged soft sphere model at c_{st}=0.005M (22). Here a cluster is defined as a group of ions connected by bonds, where by definition any two ions whose separation is less than 2R are connected by a bond. In this model R=4.2Å. The population of the cluster is the average number of such clusters per 100 cations and 100 anions, where the averages were derived by the MC method (22). The clusters are grouped in pairs which differ only in charge reversal symmetry. No other clusters were seen in the simulation reported.

of their concentrations in a model system with no specific ion-ion interactions.

In ionic systems for which T_r=0.15, as for models for 2-2 aqueous electrolytes, the Bjerrum theory of ion pairing gives osmotic coefficients and g_{+-} at contact in quite good agreement with the HNC approximation, as shown in Figs. 2 and 3. In the HNC approximation, unlike the Bjerrum theory, nothing is assumed a priori about the structure of the solutions, i.e. about the classification of the ions into 'paired' and 'free' categories. So we need not assume that ion pairs are formed to account for the properties of such systems, as indeed was pointed out by Guggenheim some time ago (30).

Now we ask a further question, namely, is the solution structure implied by the ion pair theory correct? Of course one implication of the law of mass action applied to the 'free'-'pair' equilibrium is that for $c_{st}>K$, where K is the Bjerrum mass action constant, most of the ions are paired, the more so the higher the concentration. However this is not consistent with the HNC results (27), with recent MC results (25), nor with the conductivity data for real 2-2 aqueous electrolytes (27). Instead it seems that for $c_{st}>K$ the distinction between free ions and ion pairs tends to fade away, at least for the primitive model (27).

Another aspect that is outside of the usual ion pair picture is the surprisingly large concentration of higher aggregates found in even dilute solutions for the model systems. (Fig. 4 and references 25,27) Associated with this phenomenon are relatively large values of $g_{++}(r)$ which may play an important role in certain chemical rate processes (27).

These ion pair studies lead to the following conclusion: For ionic systems with $T_r \geq 0.1$, a chemical model based on ion pairing, such as Bjerrum's theory, may lead to erroneous conclusions regarding the structures of the solutions even when the fit of the chemical model to some solution properties is quite good, as in Fig. 2.

SECTION III - FITTING MODELS TO NON-THERMODYNAMIC DATA

The developments described next were stimulated by recent neutron diffraction studies by Prof. J. E. Enderby and his coworkers (31,32). The data from a single diffraction experiment, after some reduction, yield a linear combination of structure factors (cf. Eq. (6). We use S'_{ij} rather than S_{ij} because there is a small difference between the definition of the structure factor used here and by Enderby:

$$\sum_{i,j \text{ atomic species}} (\rho_i \rho_j)^{1/2} f_i(k) f_j(k) [S'_{ij}(k) - 1]. \qquad (18)$$

In the case of neutron diffraction the form factor $f_i(k)$ does not depend upon k but does depend upon the nuclear structure, so it is different for different isotopes of atomic species i. Thus from neutron diffraction data for solutions of given chemical composition but varying isotopic composition one can determine the individual partial structure factors in Eq. (18). In this way the function $S'_{Ni,Ni}(k) \equiv S'_{++}(k)$ in 4.4M $NiCl_2$(aq) was determined (31) with the result shown in Fig. 5. The dependence of the k-value of the first peak of $S'_{++}(k)$ upon $NiCl_2$ molarity also was determined (31) with the result that

$$k_0 \simeq 2\pi\rho_+^{1/3} \qquad (19)$$

as also shown in Fig. 5. This "Bragg's law" behavior may be taken as a signal of a lattice structure in the solution (31-33), but there is no corresponding indication in the thermodynamic or transport coefficients of a change in structure to a normal solution below some critical concentration (34-36).

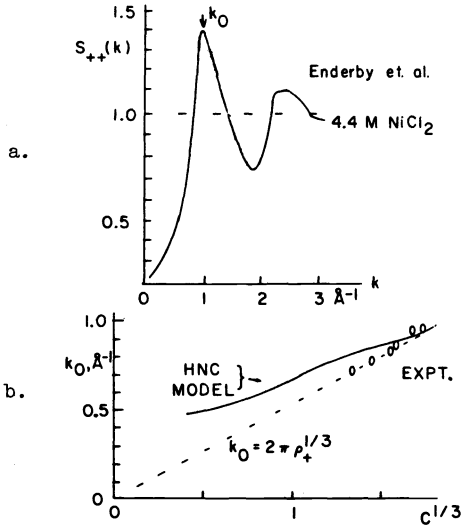

Fig. 5. a. Ni-Ni partial structure factor as determined by neutron diffraction (31,32). The location of the first peak is designated k_0.
b. Dependence of k_0 on cube root of molarity. ---, 'Bragg's law' line.
—— charged soft sphere model treated by HNC (37). Data points, neutron diffraction results of Enderby and coworkers (32).

To elucidate the molecular significance of these data we have studied MM-level models based upon Eq. (13), charged soft sphere models, with the parameters adjusted to correspond to $NiCl_2$(aq). The HNC approximation method is not reliable at the high concentrations of interest here, so we also have applied the MC method to the same models. It transpires that the structure factors calculated by the two methods are in close agreement which is strong evidence that both methods are quite accurate.

These simple models give the first peak in $S_{++}(k)$ and the concentration-dependence of k_0 in rough agreement with Fig. 5 (37). However our efforts (38) to refine the model to get good agreement with the experimental $S_{++}(k)$ in Fig. 5 have failed in a way that is most readily explained by assuming that the latter is significantly in error, even in the limited k range under the first peak.

The structural conclusion of these studies is that whether or not one wishes to ascribe the data in Fig. 5 to a lattice structure is a matter of taste. Strictly speaking, a lattice structure implies sharp lines in $S'_{++}(k)$ as a result of the long-range order. Therefore the term quasilattice is sometime used to discuss the actual situation in $NiCl_2$(aq). But

whatever a quasilattice is, it is formed from the normal or Debye-Hückel structure of an ionic solution with no hint in the thermodynamics that there is a phase transition, first order or even higher order, as expected if there is a difference in symmetry between the normal and quasilattice structures. An explicit definition of a quasilattice would imply definite characteristics in the three-point and higher correlation functions which are accessible in the model calculations when the MC simulation method is used, as illustrated for another system in Fig. 4. One could then see whether the soft-sphere model results meet these additional criteria. Unfortunately the only such explicit formulation of a quasilattice structure seems to be that due to March and Tosi (33). Since it assumes substantial inner-sphere coordination of Cl^- by Ni^{2+} in these solutions, in contradiction to the structural (32,39) and NMR (40) data, it does not seem to merit further consideration.

It seems interesting to notice that the partial structure factor as defined in Eq. (6) depends upon $g_{ij}(r)$ <u>via</u> the integral

$$\int_0^\infty 4\pi r^2 dr\, g_{ij}(r)\, \frac{\sin kr}{kr} \quad . \tag{20}$$

Depending on k the integral is more or less sensitive to $g_{ij}(r)$ in the r-range corresponding to close ij pairs. Thus it is natural to compare it with the information that may be obtained from

$$k_{ij} = \int_0^\infty 4\pi r^2 dr\, g_{ij}(r)\, \hat{k}_{ij}(r) \tag{21}$$

where k_{ij} is the coefficient of some spectral or kinetic effect that is associated with a close ij pair and $\hat{k}_{ij}(r)$ is the corresponding "local" or operator form. For example, $k_{H_2,Ne}$ may be the infrared absorption coefficient of H_2 in a mixture of H_2 with Ne or it may be the rate constant of the reaction

$$^7Li^+(m) + Ni^{2+} \rightarrow {}^7Li^+(m') + Ni^{2+} \tag{22}$$

where m→m' represents a change in the nuclear spin state of the lithium ion which may occur when it comes near the paramagnetic nickel ion (41). In both these examples there is reasonably accurate theory for the local coefficient $\hat{k}_{ij}(r)$ as required because one needs to know its r-dependence quite accurately in order to use experimental data for k_{ij} to learn about the structural quantity $g_{ij}(r)$. In the case of the Li^+-Ni^{2+} interaction in water one learns, by comparing model calculations based on Eq. (21) with experimental data for the T_1 of the $^7Li^+$, that $\bar{u}_{+,++}(r)$ for the Li^+-Ni^{2+} interaction has a sufficiently large repulsive core so that one, if not both of the ions must keep their hydration layers intact during a collision (41).

In this section we have briefly summarized two cases in which experimental data for non-thermodynamic coefficients can be combined with model calculations to characterize MM-level potentials. This procedure is complementary both to that discussed in the following Section, in which MM-level potentials are calculated from BO-level models, and to earlier work in which MM-level models were parameterized by comparison with thermodynamic data for the solutions (4,5,41).

SECTION IV - MM FROM BO

There have already been a number of fascinating studies of MM-level potentials as derived from BO-level models either by simulation (42-44,12) or by more analytical methods (45-50). These are calculations of considerable technical difficulty but in at least two cases (42 and 46, 44 and 49) there is good agreement between the simulation and analytical results for a given model. In such cases we may be confident that we know the structure at the MM level generated by the BO-level model, but to know whether the latter is realistic one requires also comparison with experimental data for relevant real solutions.

Particularly interesting for students of ionic solutions in non-aqueous solvents, particularly ion pairing phenomena, is the work of Valleau, Patey, Weis, and Levesque (42,46) concerning a BO-level model in which hard spheres with dipoles at their centers comprise the solvent while the ions are represented by charged hard spheres of the same size. If we assume 3Å diameters for the spheres then this is a model for a 1-1 electrolyte in a solvent

with dielectric constant $\varepsilon = 9.6$, hence a system with $T_r^* \simeq 0.05$. Their results are represented in Fig. 6. Compared to the primitive model with $\varepsilon = 9.6$, the present model shows far stronger +- attraction when the two ions are very close together. Clearly in the range $3\text{Å} < r < 4\text{Å}$ there is not room for a solvent molecule between the two ions so the ion-ion interaction is poorly shielded by the solvent. The extra repulsion, as much as $3k_BT$ compared to the primitive model, between the ions in the range $4\text{Å} < r < 5\text{Å}$ is more surprising. It may be noted that it is opposite in sign compared to what one would expect from the much-discussed dielectric saturation effects! It may be thought of as a consequence of the tendency of the dipolar solvent particles to stick to the ions. Finally, when the space between the ions exceeds only about one solvent diameter then the primitive model is a good approximation!

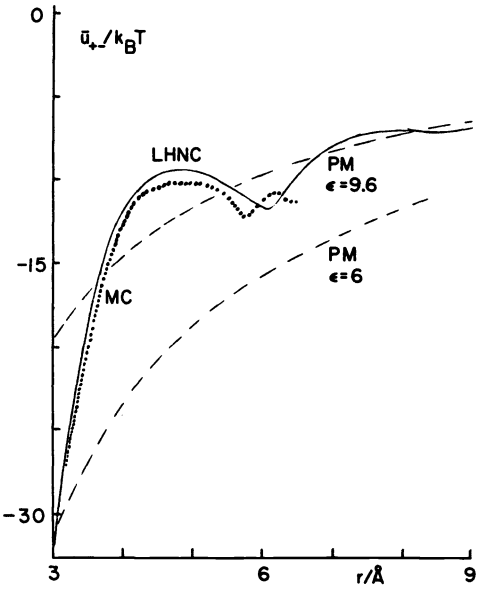

Fig. 6. Solvent-averaged potential for charged hard sphere ions in a dipolar hard sphere solvent (46). MC approximation by Patey and Valleau (42) and LHNC approximation by Levesque, Weis, and Patey (46). Also shown are the primitive model functions for solvent dielectric constants 9.6 and 6.

Comparison with some classical results makes it seem likely that the deviations from the primitive model in Fig. 6 are exaggerated compared to real systems. Thus in terms of Bjerrum's association constant, generalized to apply to any model,

$$K = F\int_R^{b/2} \exp(-\beta \bar{u}_{+-})\, 4\pi r^2 dr \qquad (23)$$

[where $b = 58\text{Å}$ is the Bjerrum length, given in Eq. (11), $R = 3\text{Å}$, and F is the conversion factor to recover K for the usual molarity scale] one finds by a crude numerical integration that the potential in Fig. 6 leads to $K = 8\times10^{10}\ M^{-1}$ while Bjerrum's theory applied to the corresponding primitive model [same R and b] gives $K = 2\times10^{5}\ M^{-1}$. In fact, to force the primitive model to agree with the larger value of K, one would have to reduce R by a factor of two. However it seems to be very well established that when ion diameters are deduced from measured ion pair association constants, especially in low-dielectric solvents, the resulting diameters quite realistic; they are not too small by a factor of two (51).

It is not known at this time what features of the hard sphere model should be changed to make it more realistic, although it may be suspected that replacement of the hard cores by soft cores, as in the change from Eq. (8) to Eq. (13), would have a big effect. This would be a very significant result because, until now, the difference between hard cores and realistic soft cores has been neglected in discussions of the physical chemistry of ionic solutions in low dielectric solvents.

Finally we turn to more recent studies by Patey, Weis and Levesque (52) for the same type of model, dipolar hard sphere solvent particles and charged hard sphere ions, but now with finite ion concentrations. These results have been obtained only by applying truncated versions of the HNC approximation to the BO-level models, so there is some uncertainty as to

whether they accurately represent the models, but it is especially interesting to discuss them because they illustrate a physical effect which has been clearly formulated only recently (50,53). We begin with an examination of the osmotic coefficients for the three models studied with T_r=0.91 (their i), 0.65 (their ii), and 0.19 (their iii). As they point out, values of T_r or equivalent ratios do not serve very well to characterize their models; for more details their paper should be consulted. However, in Fig. 7 we show a certain free energy function they obtained, and for comparison, what is found for various real solutions in water. The electrolytes in the figure are quite typical, except for those compared to T_r=0.19. For this case one wants a 1-1 electrolyte with large ions, but in such systems there seem to be well-known specific interactions, as illustrated by the large difference between Bu_4NBr and $(HOC_2H_4)_4NF$. The function plotted

$$\beta\partial\Pi/\partial\rho_+ \tilde{=} \partial(c_{st}\phi)/\partial c_{st} \qquad (24)$$

is the one given by LWP (52). Here Π is the osmotic pressure, ϕ the osmotic coefficient, $\beta=1/k_BT$, and c_{st} the stoichiometric molarity of the salt. It is the derivative of the left side, at fixed solvent concentration, that is given by LWP while the derivative on the right hand side, at fixed total pressure, has been calculated from literature data. Comparison of the two sets of curves does suggest that the models studied by LWP are not very realistic or else that the difference between fixed solvent concentration and fixed pressure is drastic. Nevertheless it is interesting to examine the structures they find, as illustrated for some examples in Fig. 8.

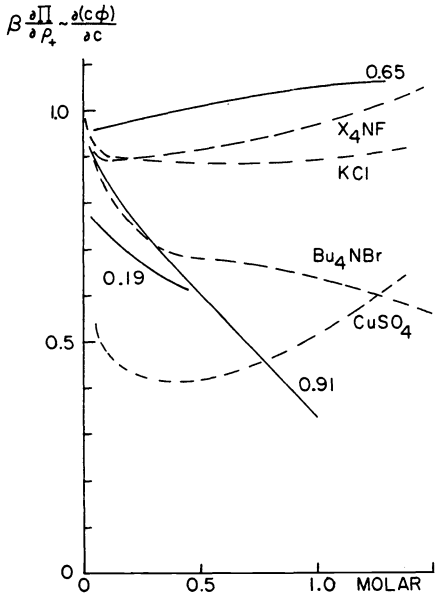

Fig. 7. Partial free energy functions for models and for aqueous solutions. The solid curves, labeled with T_r, are $\beta\partial\Pi/\partial\rho_+$ from LWP (52). The dashed curves are experimental data for $\partial(c\phi)/\partial c$ for aqueous solutions. Bu_4NBR and X_4NF (here $X=HOCH_2CH_2-$) are 1-1 electrolytes with big ions and so with nominally large T_r, perhaps as large as 0.91. For KCl (aq) we estimate $T_r \simeq 0.5$ while for $CuSO_4$ (aq) we estimate $T_r \simeq 0.15$ (cf. Fig. 1).

For the +- effective pair potential w_{+-}^{eff} (described below) we see minima in Fig. 8 corresponding to contact ion pairs and solvent separated ion pairs while smaller deviations from primitive model behavior are exhibited by the ++ pair potentials. Of course it is a challenge to try to obtain results like these for more realistic BO-level models and to try to correlate the results closely with experimental data relating to contact and solvent separated ion pairs and their rate processes. These strong features in the effective pair potentials can be accommodated in MM-level models of the type presently studied. Mainly one needs enough information, either from BO-level model calculations as in LWP or from experi-

mental data as in the preceding section, to put these consequences of the solvent structure into the models.

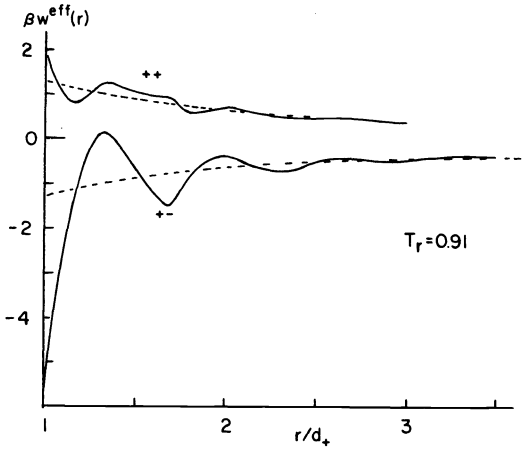

Fig. 8. Effective pair potentials (52). Solid curves, calculated by LWP (52) for T_r=0.91 model at 1M electrolyte concentration. Dashed curves; primitive model pair potentials for calculated ε_ρ.

The very new feature that is illustrated by the LWP calculations is that the effective pair potentials, such as those in Fig. 8, are dependent upon the ion concentrations. Thus the effective pair potentials [*not* the $w_{ij}(r)$ in Eq. (2)] referred to here have been defined by Adelman (53) in terms of the direct correlation functions in a way which corresponds to having exact pairwise additivity (cf. Eq. (7))

$$\bar{U}_N(\underset{\sim}{r}_1, \underset{\sim}{r}_2, \cdots, \underset{\sim}{r}_N) = \Sigma_{ij}\, \bar{w}_{ij}^{eff}(r_{ij})$$

at any one concentration, but the w_{ij}^{eff} are functions of concentration. If, for example, we keep only three point component potentials (15,54) $\bar{u}_{abs}(1,3,2)$ then the effective pair potential would be formulated as

$$w_{ab}^{eff}(1,2) = \bar{u}_{ab}(1,2) + \Sigma_s\, \rho_s \int \bar{u}_{abs}(1,3,2)\, d(3) \qquad (25)$$

which is indeed dependent on ion concentrations. In $\bar{u}_{abs}(1,3,2)$ an ion of species a is at location 1, one of species b is at location 2, and one of species s is at location 3. The new result is that the concentration dependence extends even to r=∞, where one surely has

$$w_{ij}^{eff} = e_i e_j/\varepsilon_\rho r$$

where ε_ρ is the dielectric constant, which evidently must be concentration dependent (52,53, 55). Furthermore, this ε_ρ corresponds to what one may deduce from dielectric measurements at finite frequencies (52,56). However it is still not so clear how to extract ε_ρ from such experimental data (2). Nevertheless in Fig. 9 we compare the LWP result for ε_ρ with values based upon experimental dielectric measurements (57). We see that the scale of the theoretical and experimental concentration dependence of ε_ρ is about the same, but that the pronounced curvature at small concentration, particularly for the T_r=0.91 model, has no counterpart in the typical experimental data.

The theory of ε_ρ sketched above implies that ε_ρ rather than ε_0 (i.e. ε for the pure solvent) should appear in Eq. (8) or (13) in realistic models. Therefore the effect described here is potentially very important. It will be interesting to see how this observation will be consistent with the evidence that the non-pairwise terms in $\bar{U}_N$ of Eq. (7) do not seem to have an important effect on the thermodynamic excess function. For example, Wood, Reilly, and

Robinson show that the osmotic coefficients of mixtures of more than three species of ions can be predicted accurately on the basis of data for single electrolytes and common-ion mixtures (i.e. three-ion mixtures) (58). Their results imply that pairwise additivity at the MM level is quite accurate.

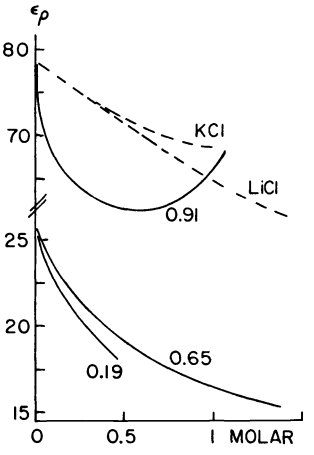

Fig. 9. Dielectric constant of ionic solution. Solid curves, labelled with T_r, are from LWP (52). Dashed curves are experimental data for aqueous solutions from Pottel (57).

Acknowledgement - We are grateful to the U.S. National Science Foundation for the support of the research reported here.

REFERENCES

1. H. S. Frank in Water, A Comprehensive Treatise, Vol. 1, p. 516, Plenum Press, New York, F. Franks, editor (1972).
2. P. G. Wolynes, Ann. Revs. Phys. Chem. 31, 1 (1980).
3. H. L. Friedman and W. D. T. Dale in Modern Theoretical Chemistry, Vol. 5, p. 85, Plenum Press, New York, B. J. Berne, editor (1977).
4. H. L. Friedman, Jour. Electrochem. Soc. 124, 421C (1977).
5. H. L. Friedman in Symposium on Thermodynamics of Aqueous Systems with Industrial Applications, American Chemical Society Symposium, M. Klein and J. Newman, editors (1980).
6. T. L. Hill, Statistical Mechanics, McGraw-Hill, New York (1956).
7. J. P. Hansen and I. R. McDonald, Theory of Simple Liquids, Academic Press, New York (1976).
8. R. O. Watts and I. J. McGee, Liquid State Physics, J. Wiley & Sons, New York (1976).
9. H. C. Andersen, Ann. Revs. Phys. Chem. 26, 145 (1975).
10. H. C. Andersen in Modern Theoretical Chemistry, Vol. 5, p. 1, Plenum Press, New York, B. J. Berne, editor (1977).
11. G. C. Lie, E. Clementi, and N. Yoshimine, J. Chem. Phys. 64, 2314 (1976).
12. W. L. Jorgensen, J. Chem. Phys. 70, 5888 (1979).
13. S. W. Harrison, S. Swaminathan, and D. L. Beveridge, J. Am. Chem. Soc. 99, 8392 (1977).
14. A. Rahman and F. H. Stillinger, J. Chem. Phys. 55, 3336 (1971).
15. W. G. McMillan and J. E. Mayer, J. Chem. Phys. 13, 276 (1945).
16. H. L. Friedman, J. Chem. Phys. 32, 1134 (1960).
17. G. R. Stell and J. Høye, Faraday Discuss. Chem. Soc. 64, 16 (1978).
18. J. Kushik and B. J. Berne in Modern Theoretical Chemistry, Vol. 6, p. 41, Plenum Press, New York, B. J. Berne, editor (1977).
19. J. P. Valleau and S. G. Whittington in Modern Theoretical Chemistry, Vol. 5, p. 136, Plenum Press, New York, B. J. Berne, editor (1977).
20. H. L. Friedman and B. Larsen, J. Chem. Phys. 69, 92 (1978).
21. N. Bjerrum, Kgl. Danske Vidensk. Selskab. 7, No. 9 (1926).
22. P. J. Rossky, J. B. Dudowicz, B. Tembe, and H. L. Friedman, J. Chem. Phys. 73, 000 (1980).
23. J. C. Rasaiah, J. Chem. Phys. 56, 3071 (1972).
24. P. J. Rossky and H. L. Friedman, J. Chem. Phys. 72, 5694 (1980).
25. J. P. Valleau, L. K. Cohen, and D. N. Card, J. Chem. Phys. 72, 5942 (1980).
26. H. L. Friedman, J. Solution Chem. 9, 371 (1980).
27. H. L. Friedman and B. Larsen, Pure and Applied Chemistry 51, 2147 (1979).

28. P. Bacelon, J. Corset, and C. deLoze, J. Solution Chem. 9, 129 (1980).
29. Y. C. Wu and H. L. Friedman, J. Phys. Chem. 70, 501 (1966).
30. E. A. Guggenheim, Disc. Faraday Soc. 24, 53 (1957). Trans. Faraday Soc. 56, 1159 (1960). A. W. Gardner and E. Glueckauf, Proc. Roy. Soc. (London) A321, 515 (1971).
31. G. W. Neilson, R. A. Howe, and J. E. Enderby, Chem. Phys. Lett. 33, 284 (1975).
32. J. E. Enderby and G. W. Neilson in Water, A Comprehensive Treatise, Vol. 6, p. 1, Plenum Press, New York, F. Franks, editor (1979).
33. G. Maisano, P. Migliardo, F. Wanderlingh, and M. P. Fontana, J. Chem. Phys. 68, 5594 (1978). N. H. March and M. P. Tosi, Phys. Lett. 50A, 224 (1974).
34. R. H. Stokes, Trans. Faraday Soc. 44, 295 (1948).
35. R. H. Stokes, S. Phang, and R. Mills, J. Solution Chem. 8, 489 (1979). R. Mills, N. H. March, P. V. Giaquinta, M. Parrinelo, and M. P. Tosi, Chem. Phys. 26, 237 (1977).
36. J. Desnoyers, private communication, 1978.
37. H. L. Friedman and J. B. Dudowicz, Aust. J. Chem. 9, 1889 (1980).
38. J. B. Dudowicz, B. Tembe, and H. L. Friedman, manuscript in preparation.
39. D. R. Sandstrom, H. W. Dodgen, and F. W. Lytle, J. Chem. Phys. 67, 473 (1977).
40. H. Weingärtner and H. G. Hertz, J. Phys. Chem. 75, 2700 (1979). H. Weingärtner, C. Müller, and H. G. Hertz, J. Phys. Chem. 75, 2712 (1979).
41. H. L. Friedman, C. V. Krishnan and L. P. Hwang in Structure of Water and Aqueous Solutions, p. 169, Verlag Chemie Gmbh., Weinheim, W. Luck, editor (1974). F. Hirata, H. L. Friedman, M. Holz, and H. G. Hertz, J. Chem. Phys., submitted.
42. G. N. Patey and J. P. Valleau, J. Chem. Phys. 63, 2334 (1975).
43. G. Palinka, W. O. Riede, and K. Heinzinger, Z. Naturforsch. 329, 1137 (1977).
44. C. Pangali, M. Rao, and B. J. Berne, J. Chem. Phys. 71, 2975 (1979).
45. L. Blum, J. Stat. Phys. 18, 451 (1978).
46. D. Levesque, J. J. Weis, and G. N. Patey, Physics Letters 66A, 115 (1978).
47. G. N. Patey, D. Levesque, and J. J. Weis, Mol. Phys. 38, 219 (1978).
48. D. Levesque, G. N. Patey, and J. J. Weis, Mol. Phys. 34, 1077 (1977).
49. L. Pratt and D. Chandler, J. Chem. Phys. 67, 3683 (1977).
50. S. Adelman and J.-H. Chen, J. Chem. Phys. 70, 4291 (1979).
51. C. A. Kraus, J. Phys. Chem. 60, 129 (1956).
52. D. Levesque, J. J. Weis, and G. N. Patey, J. Chem. Phys. 72, 1887 (1980).
53. S. A. Adelman, J. Chem. Phys. 64, 724 (1976).
54. H. L. Friedman, Molecular Physics 2, 23 (1959).
55. D. Y. C. Chan, D. J. Mitchell, B. W. Ninham, and B. A. Pailthorpe, J. Chem. Phys. 69, 691 (1978).
56. R. W. Fulton, J. Chem. Phys. 68, 3095 (1978).
57. R. Pottel in Water, A Comprehensive Treatise, p. 421, Plenum Press, New York, F. Franks, editor (1973).
58. P. J. Reilly, R. H. Wood, and R. A. Robinson, J. Phys. Chem. 75, 1305 (1971). H. L. Anderson and R. H. Wood in Water, A Comprehensive Treatise, Vol. 3, p. 119, Plenum Press, New York, F. Franks, editor (1973).

ADDENDA

In connection with Table 1 it may be remarked that quantum effects are not always neglible in BO-level models for solutions. For an example in which quantum corrections are made, see S. Goldman, J. Chem. Phys. 67, 727 (1977).

A modern version of Bjerrum's theory which captures the coexistence curve in Fig. 1 has been formulated by W. Ebeling and M. Grigo, Ann. Phys. (Leipzig) 36, 21 (1980)